Proceedings of ASME Turbo Expo 2011
GT2011
June 6-10, 2011, Vancouver, British Columbia, Canada

GT2011-45488

THE USE OF PERFORATED DAMPING LINERS IN AERO GAS TURBINE COMBUSTION SYSTEMS

Jochen Rupp*, **Jon Carrotte**
Department of Aeronautical and Automotive Engineering
Loughborough University, UK

Michael Macquisten
Rolls-Royce plc
Derby, UK

ABSTRACT

This paper considers the use of perforated porous liners for the absorption of acoustic energy within aero style gas turbine combustion systems. The overall combustion system pressure drop means that the porous liner (or 'damping skin') is typically combined with a metering skin. This enables most of the mean pressure drop, across the flame tube, to occur across the metering skin with the porous liner being exposed to a much smaller pressure drop. In this way porous liners can potentially be designed to provide significant levels of acoustic damping, but other requirements (e.g. cooling, available space envelope etc) must also be considered as part of this design process.

A passive damper assembly was incorporated within an experimental isothermal facility that simulated an aero-engine style flame tube geometry. The damper was therefore exposed to the complex flow field present within an engine environment (e.g. swirling efflux from a fuel injector, coolant film passing across the damper surface etc.). In addition, plane acoustic waves were generated using loudspeakers so that the flow field was subjected to unsteady pressure fluctuations. This enabled the performance of the damper, in terms of its ability to absorb acoustic energy, to be evaluated. To complement the experimental investigation a simplified 1D analytical model was also developed and validated against the experimental results. In this way not only was the performance of the acoustic damper evaluated, but also the fundamental processes responsible for this measured performance could be identified. Furthermore the validated analytical model also enabled a wide range of damping geometry to be assessed for a range of operating conditions. In this way damper geometry can be optimized (e.g. for a given space envelope) whilst the onset of non-linear absorption (and hence the potential to ingest hot gas) can also be identified.

NOMENCLATURE

A	Area
C_D	Discharge coefficient
c	Speed of sound
D	Orifice diameter
f	Frequency
H	Combustor height (main duct height and width)
L	Damper length
$\dot{m}$	Mass flow
M	Mach number
NL	Normalised acoustic energy loss
p	Pressure
p'	Fluctuating pressure
R	Reflection coefficient
r	Orifice radius
S	Distance between damping and metering skin
St	Strouhal number ($\omega r / u$)
t	Aperture thickness
U	Mean velocity at end of vena contracta
u	Mean velocity in plane of aperture ($u = U\, C_D$)
V	Volume
v	Fluctuating velocity
W	Damping liner width
x	Radial coordinate
y	Axial coordinate
Γ	Inertia term in the Rayleigh Conductivity
γ	Ratio of specific heat capacities
δ	Resistance term in the Rayleigh Conductivity
η	Liner compliance
Π	Acoustic energy flux
Π_L	Acoustic energy loss
ρ	Density

* On secondment from Rolls-Royce plc

σ Porosity total area of apertures divided by LW
ω angular frequency (2πf)

Subscripts

i Incident wave component
r Reflected wave component
1 Denotes damping skin
2 Denotes metering skin

Superscripts

\+ Downstream travelling wave
\- Upstream travelling wave
^ Complex amplitude
' Fluctuating quantity

1. INTRODUCTION

Gas turbine combustion systems are susceptible to thermo-acoustic instabilities because of the potential for unsteady heat release. Thermo-acoustic instabilities can lead to large acoustic pressure oscillations which can damage the combustion system. Furthermore, the lean operating conditions associated with modern, low emission, combustion systems mean that these systems are more susceptible to such instabilities. However, one strategy by which instabilities can be avoided is to increase the absorption of acoustic energy (i.e. damping) within the combustion system through the use of passive damping devices. An example of one such device is a perforated plate which (typically) incorporates a uniform array of orifices through which a mean (or bias) flow is passed.

1.1 Single Orifice Acoustic Absorption

Several investigators have considered the flow through a perforated liner with bias flow and the ability to obtain dissipation of acoustic energy over a wide frequency bandwidth. For example, Heuwinkel et al. [1] have undertaken experimental measurements on such devices whilst Eldredge and Dowling [2] have conducted both experimental and theoretical investigations. By assuming that the orifices within the porous plate are sufficiently separated (i.e. so that they behave as if in isolation), then work undertaken on single orifices can be used to help understand the performance of perforated liners. For a single orifice absorption is achieved via the unsteady flow that is generated through the liner holes by the acoustic pressure oscillations.

In the case of linear absorption the amount of energy absorbed, relative to the incident acoustic energy, is constant. Howe [3] developed a linear absorption model for a single orifice within a *thin* plate. This was based on the shedding of unsteady vorticity, from around the rim of the hole, due to oscillation of the flow passing through the orifice. In this way acoustic energy is transferred into the kinetic energy of the velocity field which is then dissipated into heat by turbulent dissipation. In addition to the unsteady pressure drop across the orifice, the model indicates the amount of energy absorbed is a function of Strouhal number ωr/u (Figure 1) i.e. the frequency of the incident acoustic wave, mean flow velocity in the plane of the orifice and the orifice radius.

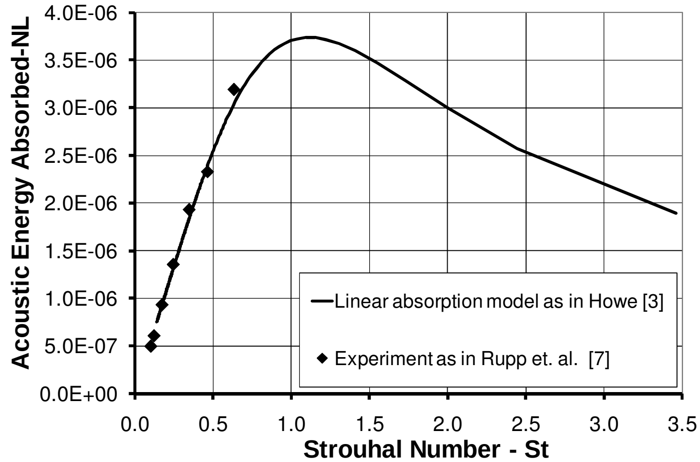

Figure 1: Acoustic energy absorption by a single orifice [7]

Many authors have considered the acoustic energy dissipation through holes or liners ([2], [4]-[6]) using linear absorption based models such as that developed by Howe [3]. However, it should be noted that when the fluctuating velocity introduced by the acoustic pressure oscillations is comparable with the mean velocity of the flow through the holes then non-linear absorption is observed ([6]–[9]). In this case the amount of energy absorbed, relative to the incident energy, is no longer constant but is a function of the amplitude of the incident acoustic wave. Furthermore differences in the oscillating flow field features, that account for this absorption characteristic, mean that linear absorption models are no longer applicable (i.e. a different type of model is required). Experimental measurements by Rupp et. al. [7,10] have indicated the different absorption regimes (Figure 2).

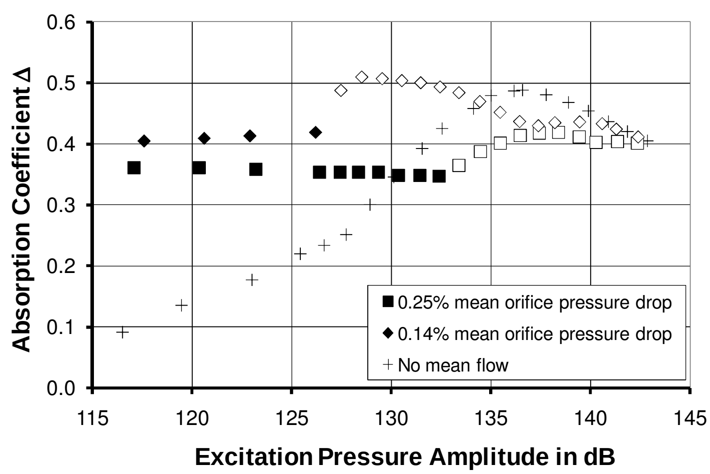

Figure 2: Measured linear and non-linear absorption characteristic of a single orifice [7]

Note that in the data presented above the solid and hollow symbols are used to identify the linear and non-linear absorption regimes respectively. Hence for a given mean pressure drop (Δp/p) across an orifice (and hence mean velocity through it), it can be seen that with increasing amplitude of the incident acoustic wave the absorption eventually goes from linear to non-linear. This transition, of course, varies with mean pressure drop (with absorption always being non-linear for the case with zero pressure drop). Such tests have been done for a range of orifices and operating conditions, with the data also confirming the absorbed energy within the linear absorption range being a function of Strouhal number (Figure 1).

1.2 Combustion System application

Most experimental and theoretical investigations have considered the performance of perforated liners within a simple 1D duct type flow or impedance tube. However, considered here is the application of a perforated liner to aero style gas turbine combustion systems. The liner is most effective when it is directly coupled to the heat release region so that it is exposed to relatively high acoustic amplitudes. However, this means that various other design constraints must be considered:

- The liner surface will be exposed to a relatively complex flow field. For example, this could include an impinging swirling fuel injector flow, the passage of a coolant film across the liner surface etc. This could potentially influence the unsteady flow field, the generation of vorticity by the liner and hence the acoustic energy being absorbed.

- The perforated liner will form part of the flame tube liner (Figure 3). However, the pressure drop across this liner is dictated by the fuel injector and the need to generate sufficient turbulent mixing of the air and fuel passing through it. A perforated liner exposed to this same pressure drop would result in a very high mean (bias) velocity through the orifice and hence a very low Strouhal number and poor absorption (see Figure 1). As a consequence an additional metering skin is required to reduce the pressure drop and control the amount of bias flow and hence the Strouhal number of the individual orifices. This double skin system must be incorporated within a limited space envelope.

- The flame tube liner cooling requirements dictate a certain level of cooling flow, per unit surface area, to maintain the structural integrity of the liner material. This means the number and size of the orifices, within the perforated liner, must consider both cooling and acoustic absorption requirements.

This paper describes an isothermal experiment in which a single sector of a gas turbine aero-engine style combustor is simulated. A passive damper which consists of a porous liner and metering skin can be incorporated into the flame tube liner. Axial acoustic waves are generated by loudspeakers and passed into the combustor test section. Based on the magnitude of the incident and reflected waves an assessment can be made of the acoustic energy being absorbed in this relatively complex environment. A simplified analytical model is also developed and validated against the experimental measurements. In this way the observed acoustic performance can be related to the fundamental processes generated by the incident acoustic waves. Furthermore the validated acoustic model enables the performance of a wide range of acoustic geometry, at a variety of operating conditions, to be investigated.

2. EXPERIMENTAL FACILITY

The facility is designed to be a simplified single sector representation of an annular type combustor, the geometry being broadly representative of a lean burn type system. A fuel injector is mounted on the end of a square acrylic duct of height H (Figure 3). The damper section consists of a width W and length L. An aperture of size $W \cdot L$ on one wall of the duct, immediately downstream of the fuel injector, enables various passive damper assemblies to be inserted. This simulates the presence of a passive damper in the inner (or outer) wall of a flame tube. The parameter S represents the distance between the damping and the metering skin.

Atmospheric air is drawn through the fuel injector and damper assembly, whilst holes and slots within the injector mounting plate also simulate the presence of a starter film passing over the damper surface. The presence of the fuel injector and starter films etc are thought to generate a reasonable isothermal representation of the complex flow field to which the passive damper would be exposed within an engine environment. Having passed through the test section this flow then continues down the duct before issuing into a plenum and exhausting to atmosphere via a centrifugal fan. Typical operating conditions correspond to a 3% pressure drop (Δp/p) across the fuel injector and damper.

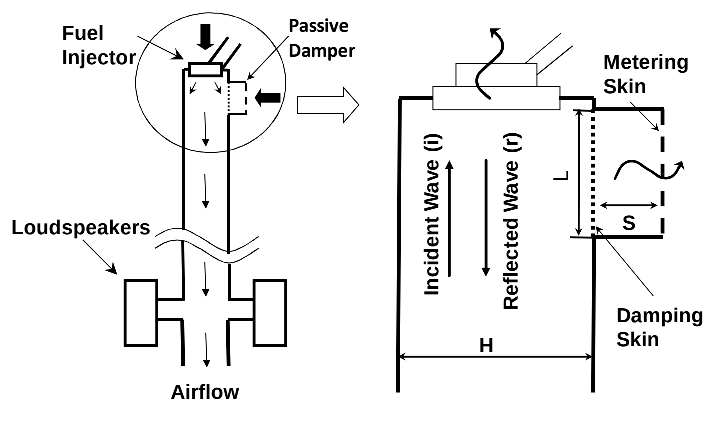

Figure 3: Schematic of test facility

The damper consists of two skins or liners and its design highlights some of the conflicting requirements associated with operating a porous liner in a gas turbine combustion environment. The relatively high pressure drop across the flame tube liner indicates potentially high velocities through any orifices (and hence low Strouhal numbers). To increase the Strouhal number to a point where, as indicated by Howe [3], some acoustic absorption will take place would require orifices of relatively large diameter. However, this would result in an unacceptably high flow rate for the combustion system. Consequently the passive damper consists of two skins in which the outermost liner is the metering skin. As its name suggests this meters or controls the flow through the damper and hence most of the mean pressure drop occurs across this skin. In this case the skin contains a porosity (i.e. open orifice area to skin surface area) of $\sigma_2 = 1.23\%$ with apertures of 1.0mm diameter. The inner layer is the damping skin containing a porosity of $\sigma_1 = 3.56\%$ with apertures of 0.7mm diameter. This distribution of porosity causes most of the flame tube liner mean pressure to occur across the metering skin (~2.7%Δp/p) with a much smaller mean pressure drop across the damping skin (~0.3%Δp/p). Hence a large number of small diameter holes can be used to obtain appreciable acoustic absorption. However, it should be acknowledged there is a compromise between the amount of bias flow available, the need to keep the liner cool and the amount of acoustic absorption that can be achieved.

Unsteady acoustic pressure fluctuations are generated by a similar system to that described by Barker et al.[11]. Two JBL 600 Watt Loudspeakers connected towards the downstream end of the duct are used to generate plane acoustic waves within the duct (Figure 3). These loudspeakers are driven by a Chevin Research A3000 amplifier system and can generate plane acoustic waves over a wide range of frequencies. In addition to the instrumentation required for monitoring and controlling the test rig, four fast response transducers could be positioned at any axial location within the downstream duct. The information from these transducers was processed using the 'two microphone' technique outlined by Seybert and Soernarko [12]. Based on any two of the pressure measurements the complex amplitudes associated with the acoustic waves travelling towards, and being reflected away from, the combustor test section (i.e. the incidence and reflected waves) could be determined. In addition, similar fast response transducers enabled time resolved pressure measurements to be made in the cavity between the passive damper skins. The time resolved data was captured at a frequency of 40kHz, with 32768 samples being collected for each one of eight data blocks. Both static and, where applicable, dynamic calibrations were performed on the instrumentation used. Repeatability tests suggested that all pressure measurements were repeatable to better than 5Pa whilst derived quantities, such as reflection coefficient, were repeatable to +/- 1%.

The acoustic test conditions were chosen to be representative of those conditions likely to be of interest at engine conditions (when appropriately scaled). Hence acoustic frequencies were in the range of 250Hz to 350Hz (and well below the cut-on frequency associated with any higher order duct modes). At engine operating conditions these frequencies correspond to a range of 430Hz to 600Hz based on Strouhal number scaling and assuming a compressor delivery temperature of order 900K. The acoustic amplitudes within the test section were approximately 135dB and represents approximately 3% of the liner mean pressure drop. For the same non-dimensional pressure drop this corresponds to an amplitude of order 165dB within an engine in which the combustion inlet pressure is 40bar.

3. EXPERIMENTAL RESULTS

Whilst many porous liner studies have been undertaken within relatively simple 1D type geometries the current investigation is aimed at exploring the performance of such devices in more complex geometries. As an example the mean static pressure distribution measured on the face of the damping skin is presented (Figure 4). The contours show the static pressure in relation to the mean pressure drop across the damping skin. Note the highly non-uniform distribution being measured on the face of the damper. A high static pressure is observed where the efflux from the injector impinges onto the passive damper, this pressure being greater than the design pressure drop across the damping skin. In other words at this location the pressure on the damper face, inside the flame tube, is greater than the pressure within the cavity between the porous liners. This must give rise to some concern regarding the ingestion of hot gas into the cavity between the damping and metering skins. As fluid accelerates away from the impingement point the static pressure drops so increasing the pressure drop across the damping skin. On a spatially averaged basis the damping skin is designed to operate in a linear absorption regime such that any fluctuations in velocity associated with the acoustic pressure oscillations is less than the mean velocity through the orifices. However, on a local basis the measurements suggest that, potentially, this may not be the case.

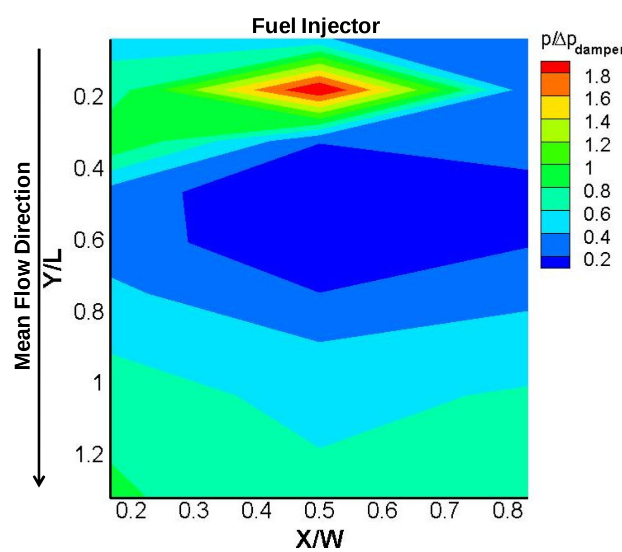

Figure 4: Mean pressure distribution along damper surface

With the loudspeakers activated a typical mode shape is presented (Figure 5), this being normalized by the maximum pressure amplitude. As to be expected in all cases a pressure anti-node is located close to the downstream face of the injector. Thus the proximity of the damper to the fuel injector means that the damper is also exposed to a region of high pressure fluctuations, although these fluctuations will reduce towards the damper trailing edge. This variation is a function of the acoustic wavelength relative to the damper length. From data such as this the magnitude of the acoustic waves travelling towards, and away from, the test section can be calculated. In terms of an energy budget the acoustic energy travelling towards the test section can either (i) pass through the fuel injector, (ii) be absorbed by the damper, or (iii) be reflected back down the duct. The ratio between the incidence and reflected acoustic energy is indicated by the reflection coefficient i.e.

$$R = \frac{p_r^2}{p_i^2}.$$

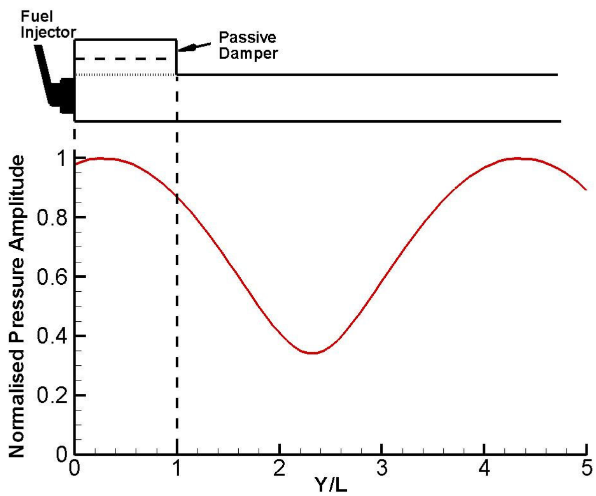

Figure 5: Pressure amplitude mode shape example

Initially the reflection coefficient was measured over a range of frequencies for the case where the damper was replaced by a solid surface (Figure 6). In this case the difference between the incident and reflected acoustic energy reflects that portion of the acoustic energy that is being transmitted through the fuel injector. For example, at 300Hz the results indicate approximately 35% of the incident energy is reflected back down the duct, with the remaining energy (65%) exiting the test section through the fuel injector. In addition, results are also presented with the passive damper present in which the gap between the two skins was set to its datum value (S/H = 0.125). Note that other tests performed at smaller gaps also indicated a similar reflection coefficient. The reduction in reflected energy is associated with the inclusion of the passive damper assembly and the absorption of acoustic energy by the damper. However, additional tests were also performed in which the damping skin was removed and only the metering skin was present (placed flush with the inside surface of the duct). Note the similarity in the reflection coefficient over the range of frequencies tested. This suggests that for this datum configuration the acoustic energy absorption was associated with the metering skin, with no acoustic energy being absorbed by the damping skin. However, further measurements were undertaken with the passive damper in place but where the gap between the two liners was increased, in various increments, from 0.125 ≤ S/H ≤ 1.46 (Figure 7). It can be seen that with an increasing gap the amount of reflected energy decreases until, at the larger separations, virtually no acoustic energy is being reflected back from the test section. In other words for these configurations the results suggest a relatively large amount of acoustic energy is being absorbed.

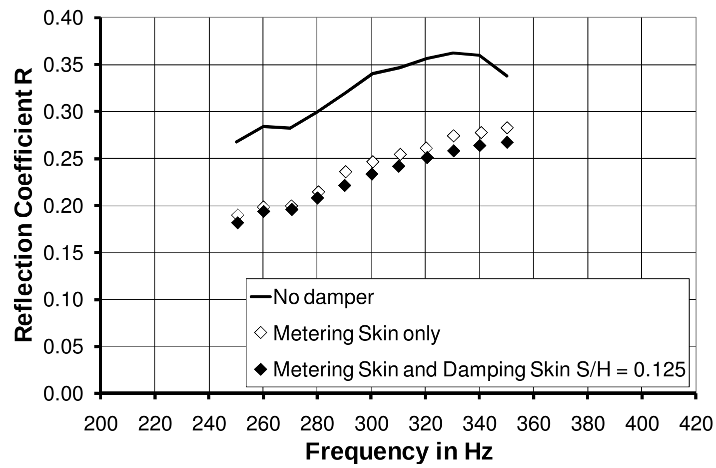

Figure 6: Comparison of measured reflection coefficients

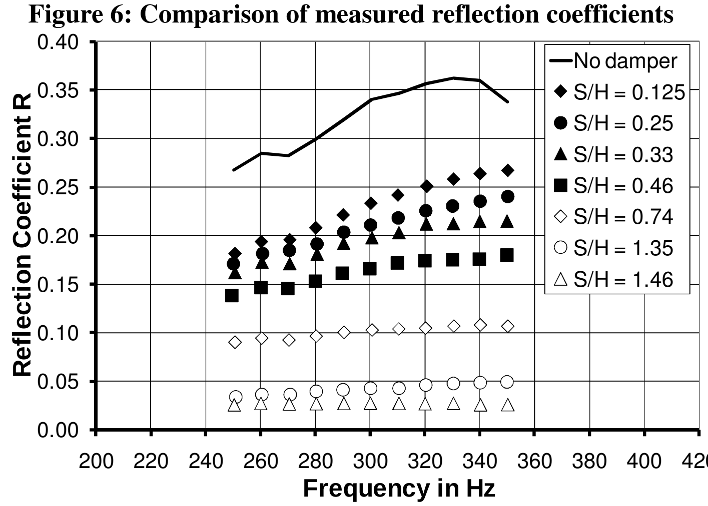

Figure 7: Reflection coefficients of various liner separations

4. ANALYTICAL MODEL

To enable interpretation of the experimental results a simple 1D analytical model was developed. The model is intended to be used as a rapid passive damping design tool to optimize acoustic absorbers for gas turbine combustors. The model assumes that the acoustic wavelength is much greater than the liner length (i.e. a 'long wavelength' assumption) so that a uniform fluctuating pressure ($p_0'(y) = const$) is imposed on the face of the damper (Figure 8).

This fluctuating pressure generates velocity perturbations leading to fluctuations in (i) the mass flow entering ($\dot{m}_{in}$) and leaving ($\dot{m}_{out}$) the volume between the damping skins and (ii) fluctuations in pressure inside the cavity (p_1'). Hence the time dependent mass flow variation inside the volume (V) between the skins is.

$$\frac{dm}{dt} = V\frac{d\rho}{dt} = \dot{m}_{in}' - \dot{m}_{out}' . \quad (1)$$

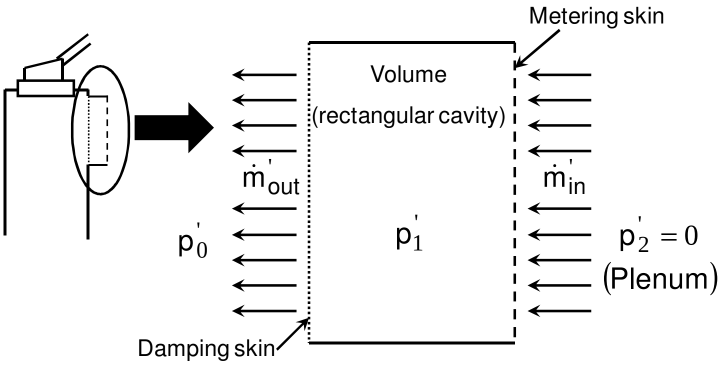

Figure 8: Schematic of analytical model

Assuming isentropic fluctuations ($p'/\bar{p} = \gamma\, \rho'/\bar{\rho}$) then

$$(j\omega)V\gamma\bar{\rho}_1 \frac{p_1'}{\bar{p}_1} = \dot{m}_{in}' - \dot{m}_{out}' \quad (2)$$

where $\rho' = \hat{\rho}\exp(j\omega t)$, $\dot{m} = \hat{m}\exp(j\omega t)$ etc. Note that it is assumed the gap between the skins is not of sufficient size to result in the generation of mode shapes within the damper cavity (i.e. uniform properties within the cavity). Hence it can be shown that:

$$\hat{p}_1 = \frac{\bar{p}_1}{\bar{\rho}}\gamma\frac{1}{V}\frac{1}{j\omega}\left[\dot{m}_{in}' - \dot{m}_{out}'\right] = \frac{\bar{p}_1}{\bar{\rho}}\gamma\frac{1}{V}\frac{1}{j\omega}\left[\bar{\rho}A\hat{v}_2 - \bar{\rho}A\hat{v}_1\right]. \quad (3)$$

The area A is defined as the damper geometric area A = LW whilst $\hat{v}_1$ and $\hat{v}_2$ are the unsteady velocities associated with the 1st (damping) and 2nd (metering) skin. These are defined as

$$\hat{v}_1 = \frac{\eta_1}{j\omega}\frac{\bar{c}^2}{L}\left[\frac{\hat{p}_1}{\gamma\bar{p}_1} - \frac{\hat{p}_0}{\gamma\bar{p}_0}\right] \quad (4)$$

$$\hat{v}_2 = \frac{\eta_2}{j\omega}\frac{\bar{c}^2}{L}\left[-\frac{\hat{p}_1}{\gamma\bar{p}_1}\right]. \quad (5)$$

It can be seen that the unsteady velocity across the damping skin is, not surprisingly, a function of the incident pressure fluctuation ($\hat{p}_0$) as well as the pressure amplitude inside the cavity ($\hat{p}_1$). Across the metering skin the unsteady velocity is only a function of the pressure amplitude inside the cavity ($\hat{p}_1$). However, for each liner a compliance has also been introduced (η) which relates the unsteady pressure drop across a liner to the oscillating flow through that liner. This requires further definition.

The Rayleigh Conductivity of an orifice describes the relationship between the unsteady pressure difference across an orifice ($\Delta\hat{p}$) and the resulting mass flow ($\hat{\dot{m}}$) (or velocity) oscillation of the orifice flow field. In addition, the linear absorption model developed by Howe [3] for a single infinitely thin orifice defined the Rayleigh Conductivity as:

$$K_D = \frac{-i\omega\hat{\dot{m}}}{\Delta\hat{p}} = D\left(\Gamma + i\delta\right).$$

The parameter Γ represents the inertia of the orifice flow field and hence its ability to react to a given pressure perturbation. The parameter δ represents the resistance associated with the unsteady orifice flow field which is responsible for the absorption of acoustic energy by each orifice ([7] and [10]). Howe has shown that these parameters are only dependent on the Strouhal number (Figure 9).

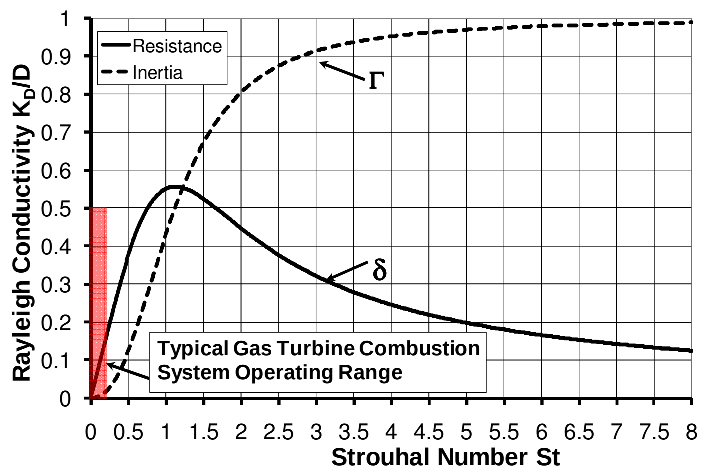

Figure 9: Rayleigh Conductivity model as in Howe [3]

Note that the Strouhal number is defined with the mean velocity in the plane of the aperture:

$$St = \frac{\omega\, r}{u} . \quad (6)$$

Conventional gas turbine combustor impingement effusion cooling systems operate at Strouhal numbers well below St = 0.25. Hence it can be seen that one option of increasing the absorption of a combustor wall is to reduce the mean velocity and hence the mean pressure drop across the wall. This will result in an increased resistance (and hence better absorption).

The described analytical model of the Rayleigh Conductivity has been incorporated into a liner compliance in a similar way to that of Eldredge and Dowling [2] so that:

$$\frac{1}{\eta}=\frac{\pi D^2}{\sigma L^2}\frac{1}{K_D}+\frac{t}{\sigma L}\,. \tag{7}$$

As equation (7) shows the conductivity has been adapted to multi-hole perforated walls by incorporating the liner porosity σ (i.e. so as to define the number of orifices present). In addition, the effect of the aperture thickness (t) on the flow inertia has also been included. The compliance parameter in equation (7) can therefore be used to calculate the velocity fluctuation across each liner due to the unsteady pressure drop (as defined in equations (4) and (5)).

The linear absorption model of Howe [3] was developed for an infinitely thin orifice where acoustic energy is absorbed via vorticity generation around the rim of the orifice. This vorticity generation is dependent on the magnitude of the velocity in this region. For an infinitely thin orifice the mean pressure drop across the orifice can be used to derive a velocity (U) and, via a hole discharge coefficient, the velocity at the rim of the orifice (u) can be obtained

$$u=U\cdot C_D\,. \tag{8}$$

However, in practical engineering applications the orifice will be located within a plate of finite thickness which will not only influence the inertia of the flow (see (7)) but also the flow velocity at the location where the vorticity is generated. In previous work [10] the acoustic absorption increased up to orifice length to diameter ratios (t/D) of 2 and then reduced from t/D=2 to 10. For orifices of this size it is thought that the resistance of the unsteady flow (and hence acoustic absorption) is still dominated by vorticity shedding at the orifice rim, but the velocity at the orifice rim (u) will vary as the orifice length is changed. For example, the hole discharge coefficient increases as t/D increases up to a value of 2 at which point the mean flow reattaches inside the orifice [13]. This increase in discharge coefficient will also reflect an increase in the velocity (u) at the orifice rim. Similarly as the orifice length is increased further (up to t/D=10) so the discharge coefficient decreases resulting in the orifice rim velocity (u) also decreasing. Further work is being undertaken to fully understand the described phenomena but for the current investigation the damping skin orifices had a t/D ratio of approximately 3. Therefore the described absorption model was calibrated against the single orifice absorption measurements in [10] for t/D ratios of 3 and the discharge coefficient was chosen accordingly.

Equations (3), (4) and (5) form a linear equation system which can be solved analytically. The model is broadly consistent with the more complex model developed by [2] but with the long wavelength assumption applied ($d/dy=0$). The absorbed acoustic energy can be calculated as [2]:

$$\Pi_L=\frac{1}{2}\rho\,\omega L^2 W\left[\mathrm{Im}\left(\frac{1}{\eta_1}\right)\left|\hat{v}_1\right|^2+\mathrm{Im}\left(\frac{1}{\eta_2}\right)\left|\hat{v}_2\right|^2\right]. \tag{9}$$

It can be seen that the acoustic energy loss calculated from equation (9) is a function of the unsteady velocities as well as the imaginary part of the compliance. Hence the acoustic absorption can be increased by increasing the unsteady velocity amplitudes across the apertures or the aperture resistances.

The acoustic energy loss is normalized with the excitation pressure amplitude ($\hat{p}_0$) as proposed in [7] and [10]:

$$NL=\frac{\Pi_L}{\left|\hat{p}_0\right|^2}\,. \tag{10}$$

This normalization makes the results independent of the applied pressure amplitude used as an inlet condition into the model.

5. MODEL VALIDATION

As part of the model validation process comparison can be made of various measured and predicted unsteady flow field characteristics.

5.1 Unsteady Pressure Drop

As suggested by equations (4), (5) and (9) the unsteady pressure drop across the damping and metering skins has a significant effect on the amount of acoustic energy being absorbed. Hence some initial validation of the model was conducted comparing the ratio of pressure amplitudes inside the cavity, $\hat{p}_1$ (i.e. between the damping and metering skins), with those within the test section, $\hat{p}_o$ (i.e. incident onto the damping skin). Space constraints meant that experimentally the cavity pressure amplitude could only be measured for liner separations greater than 0.33. However some example results are presented (Figure 10) for which measurements were available.

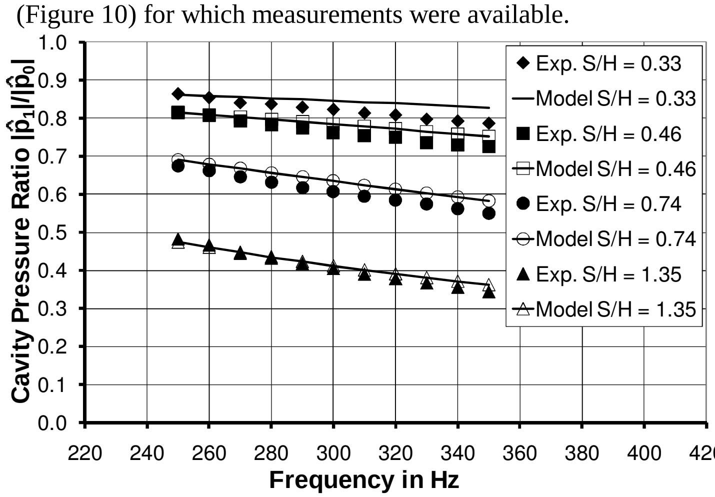

Figure 10: Cavity pressure ratio comparison between the experiment (Exp.) and the model

It can be seen that the model is able to capture the pressure ratio indicated by the experimental data. This includes the reduction in the oscillating cavity, relative to the pressure incident onto the damping surface, with increasing liner separation.

5.2 Acoustic Energy Absorption

Due to the transmission of acoustic energy introduced by the fuel injector it is not possible to directly compare the loss of acoustic energy between the experiment and the model previously presented (i.e. the model only captures the loss associated with the passive damping system and not the acoustic energy transmitted through the fuel injector). However, the model can be further validated if the fuel injector is removed and replaced by a blanking plate. As the upstream boundary condition in the test rig is now a closed end it can be assumed that the difference between incident and reflected energy is now only associated with the energy being absorbed by the passive damping system. All the experimental data compared to the modelling data in this section (Figure 11-Figure 13) has been conducted with a closed wall termination instead of the fuel injector.

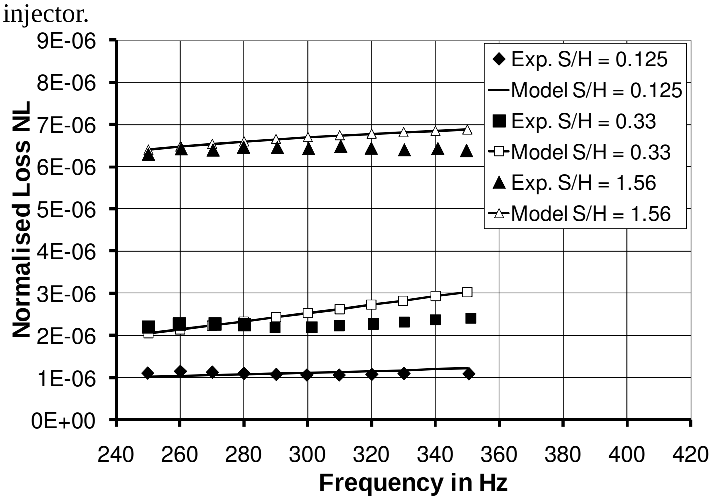

Figure 11: Comparison between predicted and measured energy loss

For this configuration three test cases have been repeated (S/H = 0.125, 0.33 and 1.56 at a $\Delta p/p$ of 3% across the two perforated skins). The acoustic energy loss has been calculated from the experiments using the difference in acoustic energy flux travelling towards and away from the test section [10], i.e:

$$\Pi^{\pm} = \frac{A}{2\rho c}(1 \pm M)^2 \left|\hat{p}^{\pm}\right|^2 .$$

With the acoustic energy loss being defined as:

$$NL = \frac{\Pi_L}{\left|\hat{p}_0\right|^2} = \frac{\Pi_i - \Pi_r}{\left|\hat{p}_0\right|^2} .$$

Then the acoustic energy loss has been normalized according to equation (10) using the maximum acoustic pressure amplitude on the face of the damper inside the main duct. This pressure amplitude was also used as input into the analytical model ($\hat{p}_0$).

Figure 11 presents a comparison between the predicted and the measured acoustic energy loss for the three test cases. It can be seen that the model is capturing reasonably well the differences in absorbed acoustic energy between configurations. However, for a given configuration there does seem to be a trend of increased discrepancies, between the measured and predicted losses, at higher frequencies. However, this may be due to errors associated with the long wavelength assumption. At relatively low frequencies the assumption of a constant pressure fluctuation across the face of the damper will be valid but this will not be the case at higher frequencies. With this in mind Figure 12 shows the measured mode shapes for 250, 300 and 350 Hz (note that the amplitudes have been normalized with the maximum pressure amplitude).

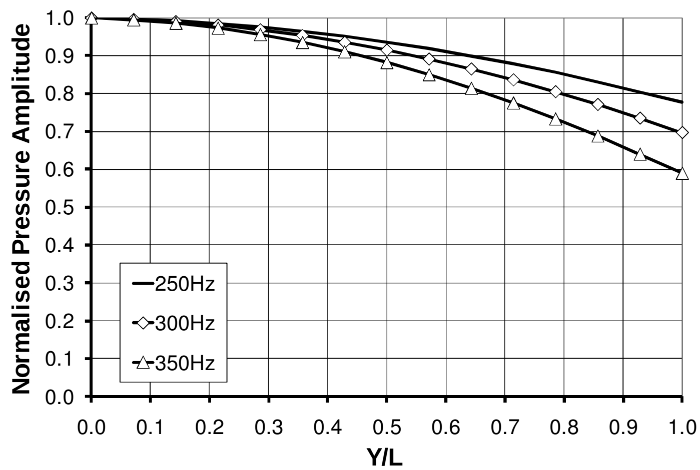

Figure 12: Normalised mode shape pressure amplitudes at various frequencies

To assess the impact of this error the measured mode shapes were used as an input to the model. The associated velocity fluctuations described in (4) have been divided into n sections with a damper length of dL = L/n. In this way the input excitation amplitude $\hat{p}_0(y)$ has been set according to the mode shape amplitudes along the y-axis, i. e.:

$$\hat{v}_{11} = \frac{\eta_{11}}{j\omega}\frac{\bar{c}^2}{dL}\left[\frac{\hat{p}_1}{\gamma\bar{p}_1} - \frac{\hat{p}_0(y_1)}{\gamma\bar{p}_0}\right]$$

$$\hat{v}_{12} = \frac{\eta_{12}}{j\omega}\frac{\bar{c}^2}{dL}\left[\frac{\hat{p}_1}{\gamma\bar{p}_1} - \frac{\hat{p}_0(y_2)}{\gamma\bar{p}_0}\right]$$

$$\vdots$$

$$\hat{v}_{1n} = \frac{\eta_{1n}}{j\omega}\frac{\bar{c}^2}{dL}\left[\frac{\hat{p}_1}{\gamma\bar{p}_1} - \frac{\hat{p}_0(y_n)}{\gamma\bar{p}_0}\right].$$

The linear equation system was then solved using the n+2 ($n \cdot \hat{v}_1, \hat{p}_1, \hat{v}_2$) equations and the acoustic energy loss then calculated and normalized in the usual way. Figure 13 shows the comparison of the experimental data to the mode shape corrected analytical absorption model. It can be seen that the model is now showing very good agreement throughout the frequency range. Hence comparison of Figure 11 and Figure 13 reflect the errors associated with the long wavelength assumption. It should be noted that when using the model for predicting damper performance the measured mode shape is not known. Hence these errors will be present at the higher frequencies although they are thought to be acceptable in terms of (i) enabling the relative performance of different damping configurations to be assessed and (ii) identifying the main factors controlling the amount of acoustic absorption.

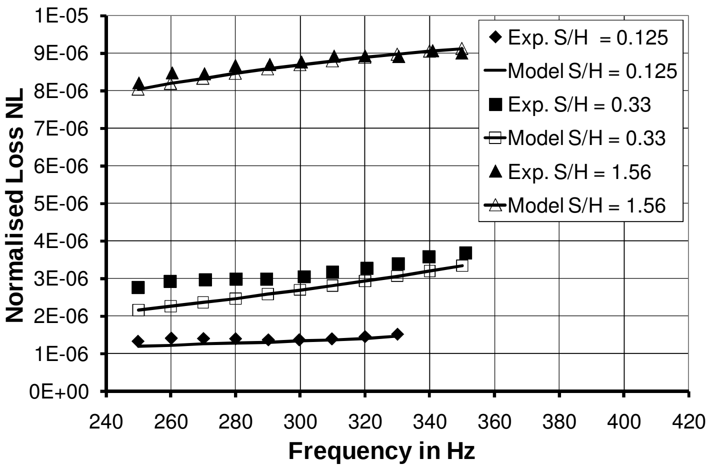

Figure 13: Comparison between experiment and modified model with pressure mode shape input function

Another interesting aspect is the application of such an analytical model to annular gas turbine combustor geometries. In this case the pressure excitation can be caused by a circumferential wave travelling through the combustor annulus geometry. The developed analytical model would be valid for a circumferential moving pressure wave where the wavelength in the circumferential direction is much larger than the width of the damper in circumferential direction.

6. DAMPER PERFORMANCE ASSESSMENT

Both the experimental measurements and analytical model have been used to relate the observed absorption characteristics with the unsteady flow field generated by the incident acoustic waves.

For aero-type applications there is a desire to minimize the space occupied by the damping system so resulting in a relatively small separation, or volume (V), between the metering and damping skins. However, this small volume means that the pressure inside the cavity is sensitive to any changes in mass flow. Hence the incident acoustic pressure fluctuation will cause a change in mass flow, through the damping skin, which quickly leads to a change in the cavity pressure (i.e. due to the small volume). In reality this means the unsteady cavity pressure approximately equals the unsteady incident pressure. Hence the unsteady pressure drop across the damping skin is minimal. This is suggested both by the experiment data already presented (Figure 6 and Figure 7), and also the cavity pressures generated by the analytical model that have been plotted for an excitation frequency of 250Hz (Figure 14). The experimental data measured in the presence of the fuel injector flow field was also added into Figure 14 for comparison. Moreover the phase between the cavity pressure and the excitation pressure in Figure 15 shows that the fluctuations for small volumes occur in phase i.e. as the incident pressure increases so does the cavity pressure at virtually the same instant in time. Furthermore it can be seen that the analytical model is agreeing very well with the measured phase even when the fuel injector flow field is present in the experiment.

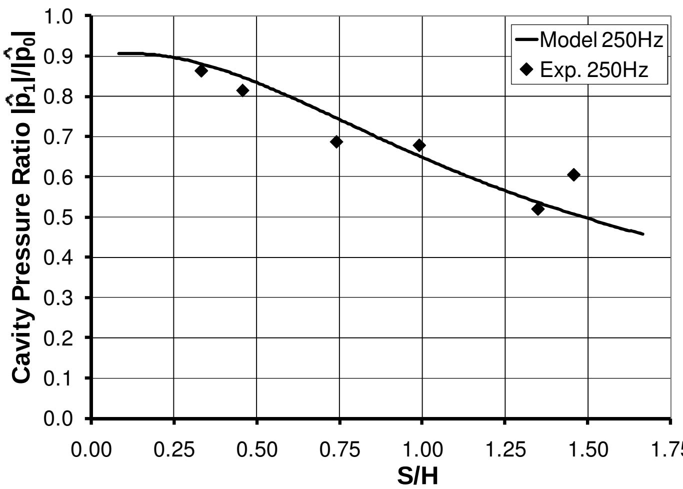

Figure 14: Cavity pressure ratio variation with liner separation, experiment with fuel injector

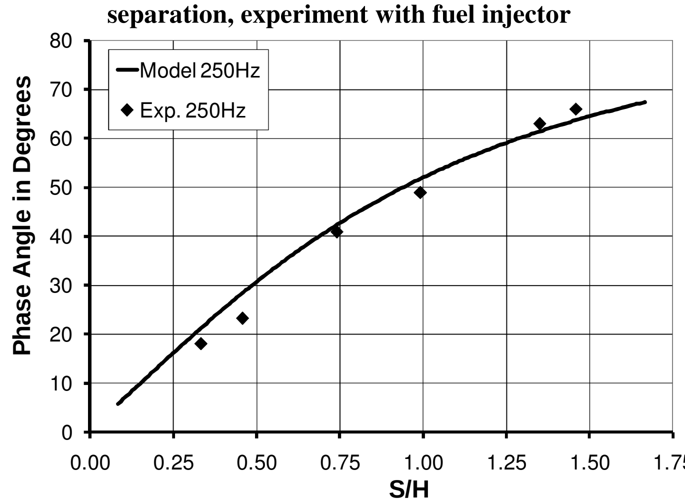

Figure 15: Phase angle between cavity pressure amplitude and excitation pressure amplitude, experiment with fuel injector

As a consequence at small cavity gaps nearly the entire unsteady pressure drop occurs across the metering skin. This explains why there was little difference in the reflection coefficient between tests undertaken with the single (metering) skin and with the damper present when the cavity gap was less than S/H = 0.125. The metering skin is designed with a high mean pressure drop and therefore the acoustic absorption generated by the metering liner is relatively small. As the gap between the skins within the passive damper increases so the volume will tend towards a plenum. In this case fluctuations in mass flow through the damping skin, due to the incident unsteady pressure, will have a limited effect on the pressure within the damper cavity (Figure 14). Consequently large unsteady pressure fluctuations and mass flow variations are generated across the damping skin enabling a significant amount of acoustic energy to be absorbed (Figure 7). This behavior is also illustrated in Figure 16 where the predicted unsteady velocities (normalised with the mean velocities across the damping and metering skins) are shown for a perturbation at 250Hz. The significant increase in the unsteady damping skin velocity with increasing liner separation can be seen. In contrast at small volumes the unsteady damping skin velocity is small and all the unsteady pressure drop is acting across the metering skin. However, because of the large *mean* pressure drop the Strouhal numbers are small and only a relatively small amount of acoustic energy is absorbed.

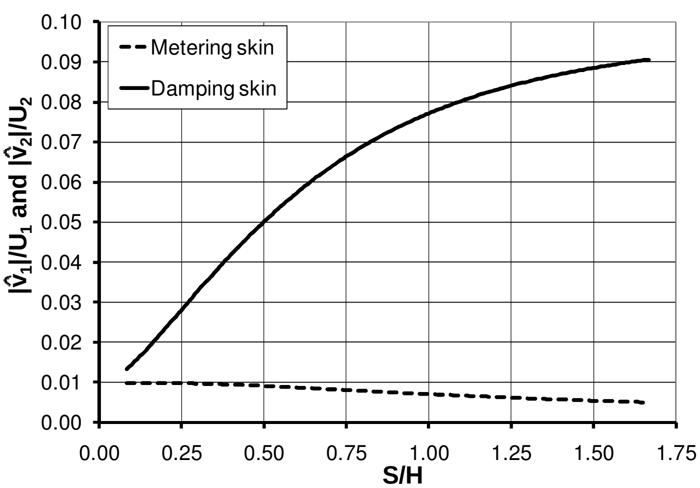

Figure 16: Unsteady velocity amplitudes with varying liner separation

In addition to understanding the physical processes associated with the damping performance, it is also worth noting the significance of the agreement between the experimental and predicted data. This data indicates that overall the absorption is linear on the face of the damper (although locally this may not be the case due to the pressure drop distribution for the cases with fuel injector). This is despite the complex flow field to which the damper is exposed.

6.1 Geometry Optimisation

In addition to understanding the unsteady flow field and the absorption characteristics the simplified model can be used to explore the impact and trade-off between various changes to the damper geometry (e.g. hole size, skin porosity etc.). For example the amount of energy absorbed, as indicated by the model, is presented for three different cavity separations and for various combinations of metering skin and damping skin porosity. These changes in porosity were achieved by varying the number of orifices within each skin. The total pressure drop across the passive damper system was kept constant as well as the mass flow through the damper.

Figure 17 presents the normalised acoustic loss with respect to a change in the mean pressure drop across the damping skin. The occurrence of the acoustic loss maxima can be explained by considering the acoustic loss defined by equation (9) as well as the velocity amplitude equations (4) and (5). The acoustic energy loss is a function of the square of the velocity amplitude and the liner compliance, the latter being dependent on the inertia and the resistance of the apertures. Moreover equations (4) and (5) show that the velocity amplitudes are calculated using the liner compliance and the unsteady pressure drop. One strategy to increase the absorption of a passive damper is to increase the resistance of the damping skin apertures by reducing the mean pressure drop across the damping skin (Figure 1 and Figure 9).

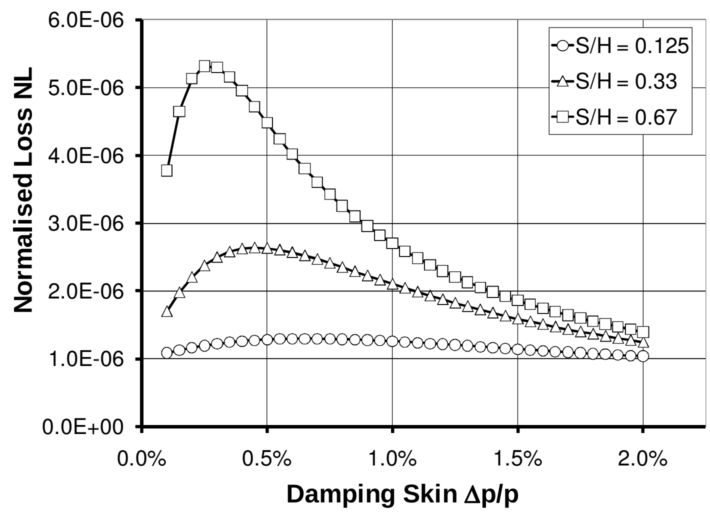

Figure 17: Normalised loss for varying damping skin mean pressure drop

However as Figure 18 shows the cavity pressure ratio, for a given volume, increases with decreasing mean pressure drop i.e. the cavity becomes more sensitive to mass flow fluctuations and so the *unsteady* pressure drop across the damping skin decreases with a decreasing mean pressure drop. Hence the possible increase in velocity amplitude, and therefore the acoustic absorption, is also accompanied by a reduction in the *unsteady* pressure drop. Consequently there is an optimum mean pressure drop across the damping skin i.e. where the acoustic absorption is at its maximum for a given cavity volume.

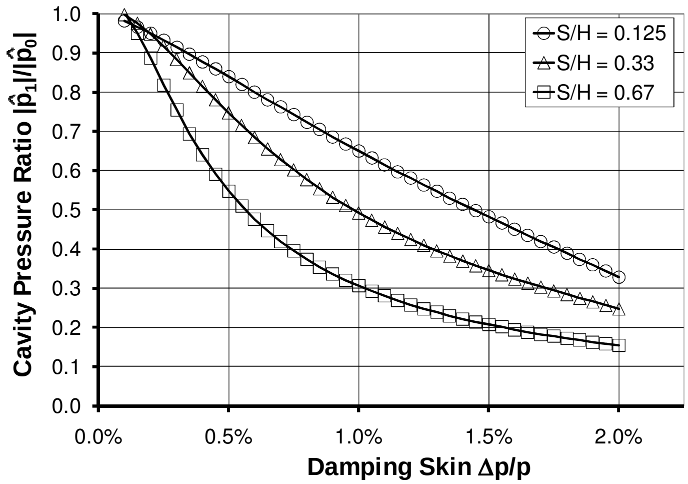

Figure 18: Cavity pressure ratio with varying damping skin mean pressure drop

6.2 Hot Gas Ingestion Analysis

Of concern with the use of passive dampers is the ingestion of hot gases from the combustor into the dump cavity. This ingestion can arise both from the time averaged and time dependent flow field characteristics.

The mean pressure drop across the damping skin means that on a spatially averaged basis the pressure within the damper cavity is greater than the flame tube pressure i.e. so relatively cool gas flows through the damping skin and into the combustor and no hot gas ingestion occurs. However, locally the mean pressure distribution will vary across the damper surface, as shown in Figure 4, resulting in the potential for hot gas to *locally* flow into the damper cavity. Hence as the mean pressure drop across the damping skin is reduced so the likelihood for local hot gas ingestion increases. However this process can be predicted by time averaged numerical (CFD) prediction of the flow field. Also of concern, though, is the time dependent ingestion of hot gas into the damper cavity due to the unsteady flow field.

As the magnitude of the unsteady pressure amplitudes inside the combustor increases so there is the potential for flow to reverse through the damping skin orifices on a time dependent basis i.e. so that hot gas is ingested at certain phases of the acoustic cycle. However, this can be investigated using the 1D analytical model in terms of

- assessing the robustness of different damper designs to gas ingestion and

- at what level of pressure oscillations within the combustor will hot gas ingestion commence.

As the velocity perturbation in the damping holes tends to the mean velocity through the holes reverse flow (and hence hot gas ingestion) will occur (i.e. $|\hat{v}_1|/U_1 \sim 1$). However, this also corresponds to the operating condition where acoustic absorption starts to become non-linear. It is known from single orifice experiments in [10] that, for a similar hole length-to-diameter ratio investigated here, non-linear absorption occurs for unsteady to mean velocity ratios of approximately 0.7 and greater. Therefore the model can be used to identify at which excitation pressure amplitudes the non-linear absorption occurs. This not only indicates the operating condition where the analytical model becomes invalid (i.e. since the linear absorption model is no longer valid), but also the operating condition where time dependent hot gas ingestion will occur.

Figure 19 shows the unsteady velocity amplitude normalized with the mean velocity across the damping skin for three different liner separations. Note that the magnitude of the excitation pressure $|\hat{p}_0|$ is normalised with the absolute mean pressure inside the main duct $\bar{p}_0$. For the largest cavity depth (S/H=0.67) it can be seen that the orifice perturbation $(\hat{v}_1)$ is of comparable magnitude to the mean orifice velocity (U_1) when the excitation amplitude is approximately 1% of the combustion chamber pressure. For example, at 40 bar this would equate to an excitation amplitude of 183dB. However as the cavity depth decreases so less acoustic energy is absorbed and the velocity perturbation $(\hat{v}_1)$ for a given excitation amplitude decreases. Hence with decreasing cavity depth the damper becomes more robust to time dependant hot gas ingestion. In this way both the relative sensitivity of different configurations to hot gas ingestion can be assessed along with the unsteady pressure amplitudes at which this will occur

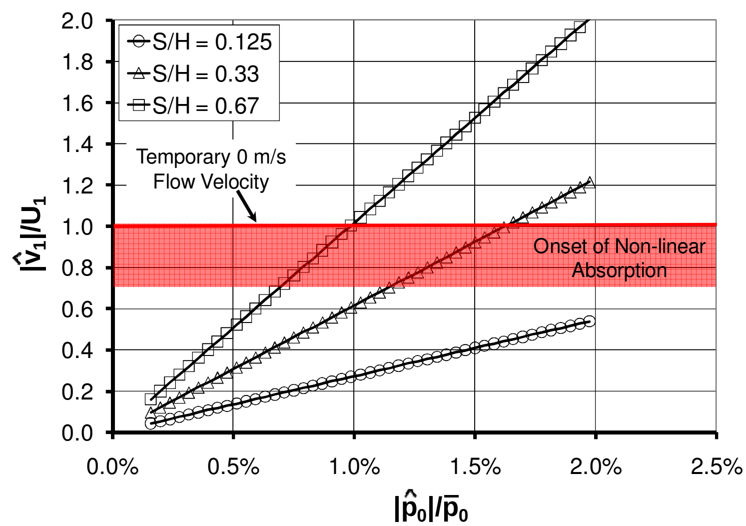

Figure 19: Estimate of pressure amplitude for hot gas ingestion

7. CONCLUSIONS

Isothermal measurements have been undertaken to assess the performance of a passive damper assembly within an aero style gas turbine combustion system. The assembly consisted of a metering and damping skin which formed part of the flame tube liner. Acoustic waves were generated via a loudspeaker system and data acquired to enable the amount of acoustic energy absorbed by the damper to be determined. In addition, a 1D linear absorption based model was developed and showed good agreement with experimental measurements.

The experimental measurements and predictions showed the unsteady pressure drop across the metering and damping skins is sensitive to the volume of the cavity between the skins. For small cavity volumes the unsteady pressure within the cavity replicates that occurring within the combustion chamber. Hence in this case the unsteady mass flow across the damping skin is small resulting in little or no absorption. Instead any absorption that does occur is associated with the metering skin where most of the unsteady pressure drop occurs. However, large cavity volumes are less sensitive to perturbations in mass flow. Hence acoustic absorption increases due to the unsteady pressure drop increasing across the damping skin. These findings are of significance to the design of combustion systems where space is often at a premium.

The simplified analytical model appears to capture the main acoustic absorption features. This suggests that the complex flow field on the face of the damping skin (impinging fuel injector flow, cooling films etc) appears to have limited influence on the overall acoustic performance. In addition, the model was also used to suggest how, within a given space envelope, the passive damper geometry required to optimize its acoustic performance. In addition, the model has also shown its potential for estimating the pressure amplitude limits at which any time dependent hot gas ingestion occurs. This also corresponds to the conditions at which non-linear absorption will take place (i.e. and so in this regime the analytical model will no longer be valid).

ACKNOWLEDGEMENTS

This research work was supported by Rolls-Royce plc and this is gratefully acknowledged by the authors. The authors would also like to acknowledge Vivek Savarianandam and Tim Bradley for their support during the project. Furthermore the support of the Loughborough University technical staff is gratefully acknowledged.

REFERENCES

[1] Heuwinkel, C., Enghardt, L. and Röhle, I. (2007) “Experimental Investigation of the Acoustic Damping of Perforated Liners with Bias Flow”, AIAA 13th Aeroacoustics Conference, AIAA 2007-3525.

[2] Eldredge, J.D. and Dowling, A.P. (2003) “The Absorption of Axial Acoustic Waves by a Perforated Liner with Bias Flow”, Journal of Fluid Mechanics, Vol. 485, pp. 307-335.

[3] Howe, M.S. (1979) “On the Theory of Unsteady High Reynolds Number Flow through a Circular Aperture”, Proceedings of the Royal Society London A, Vol. 366, pp. 205-223.

[4] Hughes, I.J. and Dowling, A.P. (1990) “The Absorption of Sound by Perforated Linings”, Journal of Fluid Mechanics, Vol. 218, pp. 299-335.

[5] Macquisten, M.A., Holt, A., Whiteman, M., Moran, A.J. and Rupp, J (2006) “Passive Damper LP Tests for Controlling Combustion Instability”, ASME Turbo Expo, GT2006-90874.

[6] Bellucci, V., Flohr, P and Paschereit, C.O. (2004) “Numerical and Experimental Study of Acoustic Damping Generated by Perforated Screens”, AIAA Journal, Vol. 42, No. 8.

[7] Rupp, J., Carrotte, J.F. and Spencer, A. (2010), “Interaction Between the Acoustic Pressure Fluctuations and the Unsteady Flow Field through Circular Holes”, Journal of Engineering for Gas Turbines and Power, Vol. 132, Issue 6.

[8] Ingard, U. and Labate, S. (1950) “Acoustic Circulation Effects and the Nonlinear Impedance of Orifices”, Journal of the Acoustical Society of America, Vol. 22, Part 2, pp. 211-218.

[9] Cummings, A (1983) “Acoustic Nonlinearities and Power Losses at Orifices”, AIAA 8th Aeroacoustics Conference, AIAA 83-0739.

[10] Rupp,J., Carrotte, J.F. and Spencer, A. (2010), “Methodology to Identify the Unsteady Flow Field Associated with the Loss of Acoustic Energy in the Vicinity of Circular Holes”, ASME Turbo Expo 2010, GT2010-22178

[11] Barker, A., Carrotte, J.F. and Denman, P. (2005), “Analysis of Hot-Wire Anemometry Data in an Acoustically Excited Turbulent Flow Field”, Expts. In Fluids, Vol.39, pp1061-1070.

[12] Seybert, A.F. and Ross, D.F. (1977) “Experimental Determination of Acoustic Properties using a Two-Microphone Random-Excitation Technique”, Journal of the Acoustical Society of America, Vol. 61, Part 5, pp. 1362-1370.

[13] Lichtarowicz, A., Duggins, R.K., Markland, E. (1965) “Discharge Coefficients for Incompressible Non-Cavitating Flow through Long Orifices”, Journal of Mechanical Engineering Science, Vol. 7, No. 2, pp. 210-219.